Role of strange quarks in quasielastic neutrino scattering

G. Garvey,* E. Kolbe, and K. Langanke
W. K. Kellogg Radiation Laboratory, California Institute of Technology Pasadena, California 91125

S. Krewald
Institut für Kernphysik, FA Jülich, D-5170 Jülich, Germany
(Received 3 May 1993)

Confirming our previous proposal, we show within a continuum random-phase approximation calculation that the ratio of proton-to-neutron neutrino-induced quasielastic yield is a sensitive way to determine the strange quark axial form factor of the nucleon. Particularly, we find that the ratio is virtually independent of final state interactions (accounted for by a finite-range force derived from the Bonn meson-exchange potential) and nuclear structure effects. We present the ratio calculated for the neutrino beam available in an experiment currently approved at LAMPF.

PACS number(s): 25.30.Pt

I. INTRODUCTION

The role of hidden flavor in the nucleon has attracted the attention of physicists for well over a decade. While deep inelastic scattering clearly reveals [1,2] the presence of gluons and strange quarks within the nucleon, we have no idea of the role these partons play in determining the properties of the nucleon. One of the most startling episodes in this saga was the possibility that strange quarks contributed one-third of the nucleon's mass. However, with the accumulation of better data and a more careful analysis of the relevant theory, the need for an unexpectedly large strange quark contribution to the nucleon mass has all but vanished [3].

More recently, the European Muon Collaboration (EMC) measurement [4] of the spin structure function of the proton implies that the axial vector coupling of a nucleon to Z^0 receives a sizable contribution from strange quarks or gluons. Their result, while surprising to some, is not inconsistent with any fundamental aspect of QCD and may well be the consequence of nonperturbative processes.

An extensive discussion of many of the issues arising from the EMC measurement and possible other strange quark contributions to the properties of the nucleon can be found in Ref. [5].

This paper will deal with a method of measuring an isoscalar contribution to the axial vector form factor of the nucleon. Following upon our earlier publication [6], we propose that this be done by comparing the yield of protons to neutrons quasielastically scattered by neutrinos from an isoscalar nucleus (e.g., ^{12}C).

*Present address: W. K. Kellogg Radiation Laboratory, 106–38, California Institute of Technology, Pasadena, CA 91125. Permanent address: Los Alamos National Laboratory, MS H846, Los Alamos, NM 87545.

II. THE NUCLEON'S NEUTRAL WEAK CURRENT

The implications of the EMC result for the neutral weak current (NWC) axial form factor of the nucleon were immediately recognized in Ref. [7]. Actually, earlier work [8–10] had anticipated that there would be "isoscalar" contributions to the NWC axial form factor. The development in Ref. [7] is carried out in terms of $SU(3)_c$ quark currents. In this paper, for convenience, we use isoscalar and isovector currents plus an explicit contribution from strange quarks. There are alternative explanations of the EMC spin structure function that employ gluonic spin contributions rather than using strange quarks. As will be indicated later in the text, the contribution we attribute to strange quarks can be ascribed to a sharing of the spin between strange quarks and gluons without affecting the analysis of our proposed measurement. As we shall assume the impulse approximation as shown in Fig. 1, the coupling of the nucleons' neutral weak current to Z^0 is crucial. Hence, that coupling is developed below.

The formalism presented appears in a few places in the literature [11,12], but is presented here to clarify the conventions used with regard to the phases and magnitudes of the various form factors that enter.

Consider the coupling of the nucleon's electric current to the photon

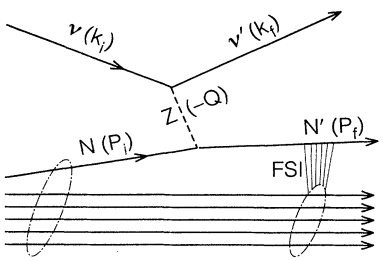

FIG. 1. Diagram showing neutrino quasielastic nucleon knockout with a final state interaction.

$$j_\mu^N \cdot A^\mu = e \left\langle N' \left| \frac{2}{3}\bar{u}\gamma_\mu u - \frac{1}{3}\bar{d}\gamma_\mu d - \frac{1}{3}\bar{s}\gamma_\mu s \right| N \right\rangle \cdot A^\mu \,, \tag{1}$$

where $|N\rangle$ is a nucleon spinor. The above quark current can be written as the following linear combinations:

$$j_\mu^N \cdot A^\mu = e \left\langle N' \left| \left(\frac{\bar{u}\gamma_\mu u - \bar{d}\gamma_\mu d}{2} \right) + \left(\frac{\bar{u}\gamma_\mu u + \bar{d}\gamma_\mu d - 2\bar{s}\gamma_\mu s}{6} \right) \right| N \right\rangle \cdot A^\mu \,. \tag{2}$$

The first term in brackets is an isovector current and the second an isoscalar [termed octet in $SU(3)_c$ parlance].

Because of our present limited ability to apply QCD, the expectation values of the quark currents cannot be calculated, so the result is expressed in terms of form factors that are extracted from data

$$j_\mu^N \cdot A^\mu = e \left\langle N' \left| F_1^N(Q^2)\gamma_\mu + \frac{iF_2^N(Q^2)\sigma_{\mu\nu}q^\nu}{2M_p} \right| N \right\rangle \cdot A^\mu \,. \tag{3}$$

Each of these form factors, the charge form factor $F_1^N(Q^2)$ and the magnetic form factor $F_2^N(Q^2)$, has an isoscalar and an isovector piece arising from the corresponding currents in Eq. (2).

Using exactly the same approach, the neutral weak current for the nucleon can be written

$$j_\mu^N \cdot Z^\mu = \sqrt{\frac{G_F}{\sqrt{2}}} \left\langle N' \left| \sum_i \bar{q}_i(1-\gamma_5)\gamma_\mu t_z q_i - 2Q_i \sin^2\theta_W \, \bar{q}_i\gamma_\mu q_i \right| N \right\rangle \cdot Z^\mu \,, \tag{4}$$

where t_z is the weak isospin, i denotes the quark flavor, (u,d,s), Q_i is the electric charge of flavor i, and θ_W is the weak mixing angle. This current can be expressed in terms of form factors as

$$j_\mu^N \cdot Z^\mu = \sqrt{\frac{G_F}{\sqrt{2}}} \left\langle N' \left| F_1^z(Q^2)\gamma_\mu + F_2^z(Q^2)\frac{i\sigma_{\mu\nu}q^\nu}{2M_p} + G_1^z(Q^2)\gamma_\mu\gamma^5 \right| N \right\rangle \cdot Z^\mu \,, \tag{5}$$

where

$$F_j^z(Q^2) \equiv \left(\frac{1}{2} - \sin^2\theta_W \right) \left[F_j^p(Q^2) - F_j^n(Q^2) \right] \tau_3 - \sin^2\theta_W \left[F_j^p(Q^2) + F_j^n(Q^2) \right] - \frac{1}{2}F_j^s(Q^2) \tag{6}$$

and

$$G_1^z(Q^2) \equiv \frac{-G_A(Q^2)}{2}\tau_3 + \frac{G_s(Q^2)}{2} \,, \tag{7}$$

where $j = 1$ or 2, $F_j^{p(n)}(Q^2)$ is the corresponding proton (neutron) electromagnetic form factor, and $F_j^s(Q^2)$ is the strange contribution to this NWC vector form factor. In like fashion, $G_A(Q^2)$ is the nucleon isovector axial vector form factor whose value (1.261 ± 0.004) at $Q^2 = 0$ is determined from neutron beta decay. Similarly, $G_s(Q^2)$ is the strange axial vector form factor. In Eqs. (6) and (7) τ_3 denotes the z component of the nuclear isospin. To simplify notation we will drop the superscript z on the weak form factors in the following.

The cross section for ν and $\bar{\nu}$ scattering from free nucleons is written as

$$\frac{d\sigma}{dQ^2} = \frac{G_F^2}{2\pi}\frac{Q^2}{E_\nu^2}\left[A \pm By + Cy^2 \right] \,, \tag{8}$$

where

$$y = \frac{4E_\nu}{M_p} - \frac{Q^2}{M_p^2} \,, \tag{9}$$

and

$$A \equiv \frac{1}{4}\left[G_A^2\left(1 + \frac{Q^2}{4M_p^2}\right) - \left(F_1^2 - \frac{Q^2}{4M_p^2}F_2^2\right)\left(1 - \frac{Q^2}{4M_p^2}\right) + F_1F_2\frac{Q^2}{M_p^2} \right] \,, \tag{10a}$$

$$B \equiv -\frac{1}{4}G_A(F_1 + F_2) \,, \tag{10b}$$

$$C \equiv \frac{1}{16}\frac{M_p^2}{Q^2}\left[G_A^2 + F_1^2 + F_2^2\frac{Q^2}{4M_p^2} \right] \,. \tag{10c}$$

In these expressions, $Q^2 = -q^2$, the relative V, A phase is $(1 - \gamma^5)$, and the explicit Q^2 dependence of all form factors is suppressed. Table I lists the form factor values at $Q^2 = 0$ for both neutrons and protons. The strange-quark form factors are, in general, not well known except that $F_1^s(0) = 0$ as the nucleon has net strangeness zero. The EMC result on the proton spin structure function can be interpreted as fixing $G_s(0) = -0.19 \pm 0.08$ [4]. While some have claimed that a Brookhaven Alternating Gradient Synchrotron νp experiment yields $G_s = -0.15 \pm 0.08$ [11], we believe this belief to be unfounded. This claimed result neglects any strange-quark contribution to the vector form factors, is strongly dependent on the value employed for the mass in the axial vector form factor, and employs a naive view of quasielastic scattering [13].

A word should be said about the Q^2 dependence of the nucleon form factors, though this will not be important for the technique proposed here, both because the momentum transfers are small ($Q^2 < 0.1$ GeV^2) and by employing ratios, the Q^2 dependence further tends to cancel. The standard dipole forms

$$G_1(Q^2) = \frac{G_A(0)\tau_3 + G_s(0)}{2\left(1 + \frac{Q^2}{M_A^2}\right)^2}, \tag{11a}$$

$$F_1^p(Q^2) = \frac{1}{\left(1 + \frac{Q^2}{M_V^2}\right)^2}\left[F_1^p(0) + F_2^p(0)\frac{Q^2}{4M_p^2 + Q^2}\right], \tag{11b}$$

and

$$F_2^{p,n}(Q^2) = \frac{F_2^{p,n}(0)}{\left(1 + \frac{Q^2}{4M_p^2}\right)\left(1 + \frac{Q^2}{M_V^2}\right)^2} \tag{11c}$$

are assumed in each case with $M = 0.843$ GeV$/c^2$ and 1.032 GeV$/c^2$ for the vector (V) and axial vector (A) form factor, respectively. For the neutron charge form factor F_1^n and the strange magnetic form factor F_2^s, we adopt the Q^2 dependences as given in [12]. $F_1^s(Q^2)$ clearly cannot be fit into this description; however, as pointed out above, $F_1^s(Q^2) = 0$ at $Q^2 = 0$, and $F_1^s(Q^2)$ has been estimated to be less than 10% of $F_2^s(Q^2)$ for $Q^2 < 0.09$ GeV^2 [12]. Furthermore, the contributions of $F_1^s(Q^2)$ are suppressed by the kinematics of the proposed experiment. Therefore, we will neglect this form factor in the following and only discuss the ratio R of proton-to-neutron yield in terms of $G_s(0)$ and $F_2^s(0)$.

TABLE I. The form factor values at $Q^2 = 0$ for both neutrons and protons.

	Proton	Neutron
F_1^z	$0.034 - F_1^s/2$	$-0.50 - F_1^s/2$
F_2^z	$1.017 - F_2^s/2$	$-0.9615 - F_2^s/2$
G_1^z	$-0.63 + G_s/2$	$0.63 + G_s/2$

III. THE NUCLEAR MODEL

In our earlier publication, the ratio R was calculated as a function of E_N, the energy of the struck-out nucleon. The results were seen to be very promising, but nuclear final state interactions were not included. In this publication these effects are considered, particularly charge exchange, which could have potentially serious effects on R.

We view the neutrino-induced nucleon knockout process as shown in Fig. 1. The incoming neutrino has an energy ϵ_i, after interacting with the nucleus it has energy ϵ_f. Before the interaction, the nucleus is in its ground state, described by the many-body wave function $|J_i T_i = 0\rangle$, where J_i stands for the total angular momentum of the state, T_i its isospin (and a set of additional quantum numbers which are omitted to simplify the notation). After the interaction with the neutrino, the nucleus is in an excited state $|J_f\rangle$ at an excitation energy $\omega = \epsilon_i - \epsilon_f$. For the case we are concerned with, $|J_f\rangle$ is a continuum state. The momentum transferred to the nucleus depends on the scattering angle θ of the neutrino and is given by

$$q = |\mathbf{q}| = \sqrt{\omega^2 + 4\epsilon_i(\epsilon_i - \omega)\sin^2\frac{\theta}{2}}. \tag{12}$$

The four-momentum transfer to the nucleus is Q, with $Q^2 = q^2 - \omega^2$. We assume a quasielastic process; i.e., the neutrino interacts only with one nucleon, while the others are viewed as spectators. In this approximation, the momentum transfer (12) is to the struck nucleon.

The cross section for neutrino- or antineutrino-induced excitation of a target state in the continuum can be derived straightforwardly by application of the usual Feynman rules and a multipole analysis of the weak nuclear current. As this has been carried out (in close analogy to electron scattering on nuclei) in detail in Ref. [14], we only state the result here:

$$\frac{d^2\sigma}{d\Omega d\omega} = \frac{G_F^2\epsilon_f^2}{2\pi^2}\frac{4\pi\cos^2\frac{\theta}{2}}{(2J_i+1)}\left[\sum_{J=0}^{\infty}\sigma_{CL}^J + \sum_{J=1}^{\infty}\sigma_T^J\right]. \tag{13}$$

The partial cross section σ_{CL}^J is defined as ($\kappa = |\mathbf{q}|$)

$$\sigma_{CL}^J = \left|\langle J_f\|\tilde{M}_J(\kappa) + \frac{\omega}{|\mathbf{q}|}\tilde{L}_J(\kappa)\|J_i\rangle\right|^2, \tag{14}$$

where $\tilde{M}_J$ and $\tilde{L}_J$ denote the multipole operators for the longitudinal (relative to q) parts of the vector and axial vector four-currents. Similarly, for the transverse cross section

$$\begin{aligned}\sigma_T^J = &\left(+\frac{Q^2}{2q^2} + \tan^2\frac{\theta}{2}\right)\\ &\times\left\{\left|\langle J_f\|\tilde{J}_J^{\rm mag}(\kappa)\|J_i\rangle\right|^2 + \left|\langle J_f\|\tilde{J}_J^{\rm el}(\kappa)\|J_i\rangle\right|^2\right\}\\ &\mp\tan\frac{\theta}{2}\sqrt{\tan^2\frac{\theta}{2} + \frac{Q^2}{q^2}}\\ &\times 2{\rm Re}\left(\langle J_f\|\tilde{J}_J^{\rm mag}\|J_i\rangle\langle J_f\|\tilde{J}^{\rm el}\|J_i\rangle^*\right).\end{aligned} \tag{15}$$

Here, $\tilde{J}_J^{\rm mag}$ and $\tilde{J}_J^{\rm el}$ are the magnetic and electric multipole operators, respectively, containing both vector and axial vector pieces. In Eq. (15), the minus sign (plus sign) refers to the neutrino (antineutrino) cross section. Following Ref. [14], the various multipole operators introduced in Eqs. (14) and (15) are expressed in terms of one-body operators in the nuclear many-body Hilbert space. The evaluation of the cross section then requires the calculation of the reduced matrix elements of these operators between the discrete initial many-body state $|J_i\rangle$ and a final continuum state $|J_f\rangle$ for a fixed energy ω. For a given exit channel (e.g., the proton or neutron channel), the excitation energy ω corresponds to the difference of E_N, the measured energy of the emitted nucleon, and E_h, the energy of the hole in the residual nucleus; i.e., $\omega = E_N - E_h$.

The nuclear model, from which we determine the initial and final many-body states, fulfills the following requirements: (1) the nuclear ground state is well described, (2) the final states are described as generic continuum states, (3) the excitation mechanism of the continuum states will be predominantly of one-particle–one-hole (1p-1h) nature, and (4) final state interactions are accounted for. These requirements are fulfilled within the continuum random-phase approximation (RPA). A detailed description of this model can be found in Refs. [15,16]. Note that in this model the continuum states fulfill the correct Coulomb boundary conditions for scattering states and an (1p-1h) excitation mechanism is explicitly assumed. The ^{12}C ground state is approximated as a Slater determinant built by Woods-Saxon single-particle wave functions. The potential parameters are chosen such to reproduce properties of the ^{12}C ground-state-like rms radius and charge form factor as closely as possible. For the hole energies we use the experimental values, thus ensuring an exact reproduction of the neutron and proton thresholds. Finally, the residual interaction employed in our calculation, which is the finite-range G-matrix interaction [17] derived from the Bonn meson exchange potential [18], has been shown to properly account for final state interactions in $(e,e'p)$ and $(e,e'n)$ reactions [19]. Results obtained in continuum RPA calculations for quasielastic electron scattering and $(e,e'p)$ scattering off ^{12}C (which, however, used a less realistic residual interaction) can be found in [16,20].

IV. RESULTS AND DISCUSSION

In this section, we present the results of our continuum RPA calculation for the neutrino-induced nucleon knockout from ^{12}C. The quantities investigated are the quasielastic cross section as a function of the kinetic energy of the struck nucleon in the final state, as well as the ratio of energy-integrated proton-to-neutron quasielastic cross sections. Particular attention is paid to the effects of the finite-range residual particle-hole interaction (final state interaction) on the ratio R.

In Fig. 2, the cross sections are plotted for quasielastic ν- and $\bar{\nu}$-induced reactions on ^{12}C as a function of the kinetic energy of the final nucleon. In this calculation, the incident neutrino energy has been fixed to $E_\nu = 200$ MeV, which is a typical value for the decay in flight (DIF) neutrino beam available at LAMPF [21]. The strange form factors are fixed at $G_s = -0.19$, taken from analysis of the proton spin structure function [4], and to $F_2^s = -0.21$ [22]. As the experimental values for the hole energies are employed, our calculation reproduces the nucleon threshold energies exactly. The difference between proton and neutron thresholds becomes apparent in the structure of the cross section at low energies, which is shifted between the proton and neutron decay channels by this energy difference (≈ 2.8 MeV). The structure is related to the isovector giant resonance structure in ^{12}C. A detailed discussion of this spectrum and its agreement with experimentally known levels is given in Ref. [15]. It is apparent from Fig. 2 that the cross section becomes essentially independent of details of nuclear structure at energies above $E_N = 30$ MeV, corresponding to nuclear excitation energy of about 45 MeV.

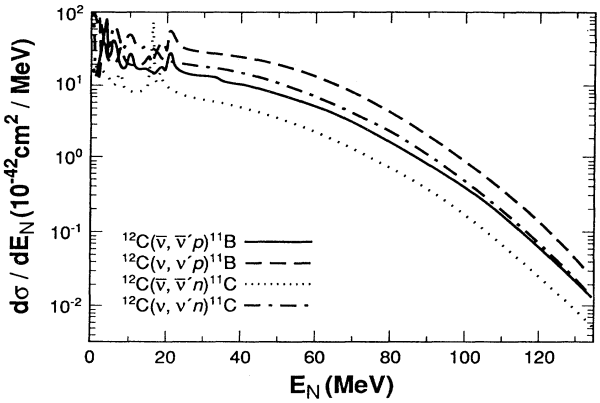

FIG. 2. Differential cross sections as a function of nucleon energy E_N for $(\bar{\nu},\bar{\nu}'p)$ (solid curve), $(\bar{\nu},\bar{\nu}'n)$ (dotted curve), $(\nu,\nu'p)$ (dashed curve), and $(\nu,\nu'n)$ (dash-dotted curve) on ^{12}C.

In an experiment [21] currently completing construction at LAMPF, it is planned to measure the proton and neutron yields for nucleons emitted with energies above 20 MeV (see below). At first glance, the structureless cross sections calculated for $E_N > 30$ MeV in the present continuum RPA approach resemble closely the one obtained in the free-response approximation (i.e., neglecting the residual particle-hole interaction) and shown in Fig. 1 of Ref. [6]. However, the inclusion of the final state interaction (FSI) increases the high energy yield as compared to the free-response calculation. Further, the relative enhancement increases with increasing nucleon energy. For example, due to final state interaction, the proton *and* neutron cross sections are increased by about 15% at $E_N = 80$ MeV, while the increase is roughly 40% by $E_N = 100$ MeV. Second, the consideration of a residual particle-hole interaction slightly changes the ratio of cross sections $\frac{d\sigma}{dE_N}(\nu,\nu'p)/\frac{d\sigma}{dE_N}(\nu,\nu'n)$ while having a somewhat larger effect on $\frac{d\sigma}{dE_N}(\bar{\nu},\bar{\nu}'p)/\frac{d\sigma}{dE_N}(\bar{\nu},\bar{\nu}'n)$ as a function of nucleon energy E_N. As shown in Fig. 3, these ratios are increased at $E_N \lesssim 100$ MeV compared

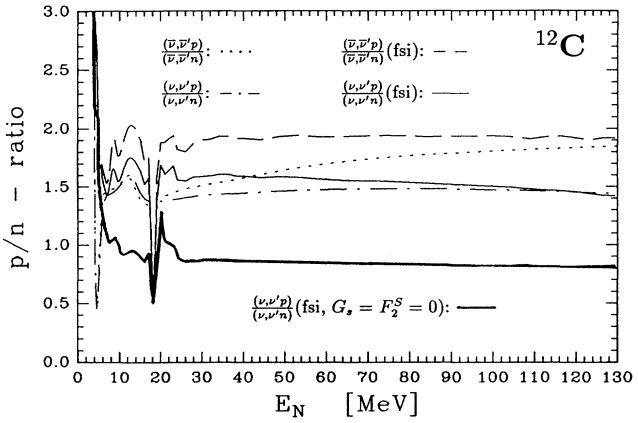

FIG. 3. Ratios of proton-to-neutron yields as a function of nucleon energy E_N. The ratios obtained in our calculation with (without) final state interaction are shown by dotted (solid) curves for antineutrino-induced reactions, while they are given by dash-dotted (dashed) curves for neutrino-induced reactions. In these calculations, we have adopted the values $G_s = -0.19$ and $F_2^s = -0.22$ for the strange form factors. For comparison, the ratio for vanishing strange form factors, calculated for neutrino-induced quasielastic knockout, is given by the lower solid curve. In this figure we have used $E_N = E_p = E_n + 2.77$ MeV.

to the calculation without residual interaction, and are slightly decreased at higher energies. It is important to realize in this figure that $E_N = E_p = E_n + 2.77$ MeV.

The effects of the final state interaction may be understood as follows: The $|T = 1\rangle$ residual interaction is repulsive (see Ref. [23]) and therefore enhances the $T = 1$ continuum at higher energies. This explains the increase of the cross sections at $E_N > 60$ MeV. However, the effect of the final state interaction on the ratio of proton to neutron yield, particularly for the ν case, is quite small. This behavior differs from electron-induced knockout reactions [19]. Here, the residual interaction significantly redistributes the yield in the final state channels, especially for the longitudinal channels. This comes about because the direct longitudinal coupling of the electron to the neutron is negligible at the mean-field level, making the consideration of final state interactions an essential ingredient in $(e, e'n)$ calculations. On the other hand, in the transverse response these effects are much less pronounced, as the electron couples to the neutron and proton at the mean-field level. Similarly, this FSI coupling between neutrons and protons is not very important in quasielastic neutrino-induced knockout reactions, noting that the latter are dominated by the isovector response function. Nevertheless, the presence of a slight redistribution of strength from the proton to the neutron channel, caused by the final state couplings of these channels, is indicated by our results in the p/n ratio.

The quantity of interest for the LAMPF experiment under construction is the total nucleon cross section [denoted by $\sigma(\nu, \nu' p)$ and $\sigma(\nu, \nu' n)$ in the following] obtained by integrating $d\sigma/dE_N$ over the energy of the emitted nucleon. Measurement of the relative yield from ^{12}C requires discrimination against protons that result from neutrino elastic scattering from the free protons in the LSND scintillator. E_m is the maximum energy that can be transferred to a free proton for the LAMPF ν beam ($E_m = 60$ MeV). Thus, this energy is used as the threshold for the ratio [19]. A fraction of the protons in ^{12}C do produce $E_p > 60$ MeV due to their Fermi motion. Using our calculated cross sections and the LAMPF DIF neutrino beam, some 800 protons will pass the threshold in 3000 h of LAMPF operation into LSND.

The dependence of the total cross section on the strange form factors can be illustrated as follows: Noting that the quasielastic neutrino-induced nucleon knockout cross section is dominated by the axial vector component, one roughly has

$$\sigma(\nu, \nu' N) \sim |-G_A \tau_3 + G_s|^2 \approx G_A^2 \left(1 \mp 2 \frac{G_s}{G_A}\right) . \quad (16)$$

Taking the value from Ref. [4], $\frac{G_s}{G_A} \cong -\frac{1}{6}$, increases the proton yield. This effect is linear with G_s. However, the ratio of proton-to-neutron yields changes appreciably:

$$R = \frac{\sigma(\nu, \nu' p)}{\sigma(\nu, \nu' n)} \approx 1 - \frac{16}{5} G_s . \quad (17)$$

Thus, this ratio is very sensitive to G_s. The measurement of the quasielastic proton-to-neutron yield appears to be a very promising way to determine the value of G_s. Furthermore, this approach has two important experimental advantages compared to experiments that determine the strange axial vector form factor from neutrino-proton scattering. While the latter is also quite sensitive to G_s [see Eq. (16)], it requires a rather precise knowledge of the absolute flux and the energy spectrum of the neutrino beam. In particular, the absolute normalization is difficult to determine experimentally, and inevitably leads to rather large uncertainties in the value of G_s determined from absolute neutrino-proton scattering experiments. Clearly, this source of uncertainty is avoided in experiments that measure the ratio of yields. As shown below, the ratio is also virtually independent of the neutrino energy for those energies present in the LAMPF neutrino beam.

The above discussion should be understood as a guideline for the realistic continuum RPA results discussed in the following. As can be seen in Fig. 4, the strong sensitivity of the ratio on the strange axial vector form factor $G_s(0)$ is confirmed as is its nearly linear dependence. However, the ratio is also dependent on the strange vector form factor F_2^s introduced by the vector–axial-vector interference term in the cross section. This is illustrated in Fig. 4, which shows the ratio as a function of $G_s(0)$ for three different values of $F_2^s(0)$. The values chosen for $F_2^s(0)$ are in the limits of the range of possible values given in Refs. [5,22]. The following features emerge: the sign of the interference term is such to increase the p/n ratio in neutrino-induced reactions. The inclusion of $F_2^s(0)$ into the Dirac form factor F_2 counteracts this trend if $F_2^s(0) < 0$, eventually changing the sign of F_2. For

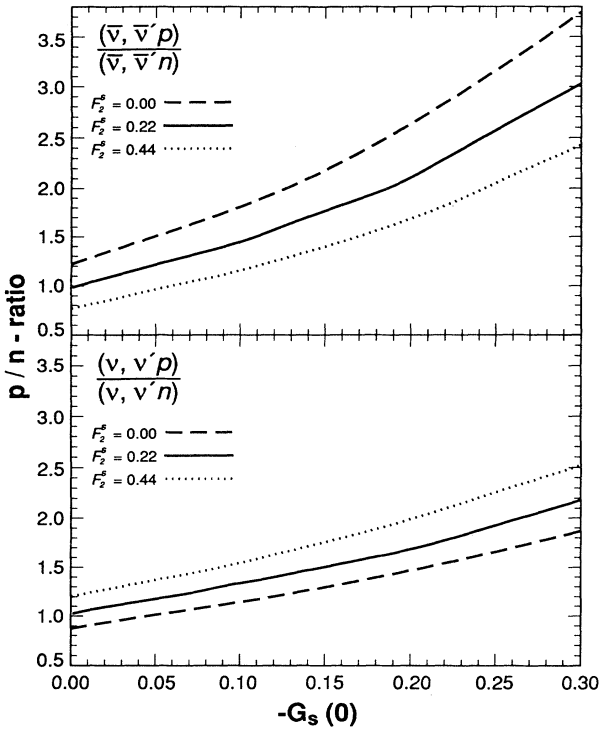

FIG. 4. Ratio of integrated proton-to-neutron yield for quasielastic antineutrino- (upper part) and neutrino-induced (lower part) reactions on ^{12}C as a function of $G_s(0)$ for different values of $F_2^s(0)$ within the theoretically estimated regime [5,22]. The incident neutrino energy was set to $\epsilon_i = 200$ MeV.

antineutrino-induced reactions, the relative sign of the vector–axial-vector interference term is reversed, hence the behavior of the ratios shown in Fig. 4. The different signs of the interference terms in $\overline{\nu}$- and ν-induced reactions are also responsible for the fact that the gradient of the ratio as a function of $G_s(0)$ is steeper in antineutrino-induced knockout reactions. In Ref. [6], the dependence of the ratio on strange form factors $F_2^s(0)$ and $G_s(0)$ has been calculated in a simple model based on free neutrino-nucleon scattering. It is remarkable that this simple model reproduces the results of these continuum RPA calculations within about 10% for the ranges of values for $F_2^s(0)$ and $G_s(0)$ considered here.

Most importantly, however, we find that the ratios are changed by less than 5% for the ranges of values for $G_s(0)$ and $F_2^s(0)$ shown in Fig. 4, if compared to those obtained in the mean-field approximation (i.e., Fig. 2 of Ref. [6]). This virtual independence of the ratio on the residual interaction confirms that the determination of the strange form factors [in particular of $G_s(0)$] from the measurement of the neutrino-induced proton-to-neutron yield will not be much affected by the influence of nuclear physics.

In an actual experiment, the neutrino beam is not monoenergetic, but rather has a broad energy distribution, and consists of a mixture of neutrinos and antineutrinos. In the following, the effects of these beam properties on the ratio of proton-to-neutrino yields are investigated, taking the LAMPF neutrino beam as an illustrative example. First, we have studied the effect of the energy distribution on the ratio. To this purpose the nucleon knockout cross sections $\sigma(\nu,\nu'p)$ and $\sigma(\nu,\nu'n)$, defined for a given incident neutrino energy, have been folded over the LAMPF neutrino energy spectrum $n_{\rm LAMPF}(E_\nu)$ [21]. With a choice for E_m ($E_m = 60$ MeV for the LAMPF beam, as discussed above), the proton and neutrino knockout cross sections relevant for the LAMPF experiment read

$$\overline{\sigma}(\nu,\nu'p) = \int_{E_m} \sigma(\nu,\nu'p)(E_\nu) n_{\rm LAMPF}(E_\nu) dE_\nu ,$$
$$\overline{\sigma}(\nu,\nu'n) = \int_{E_m} \sigma(\nu,\nu'n)(E_\nu) n_{\rm LAMPF}(E_\nu) dE_\nu , \quad (18)$$

with similar definitions for the antineutrino-induced knockout reaction cross sections $\overline{\sigma}(\overline{\nu},\overline{\nu}'p)$ and $\overline{\sigma}(\overline{\nu},\overline{\nu}'n)$. We find that the ratios of proton-to-neutron cross sections

$$\overline{R}_\nu = \frac{\overline{\sigma}(\nu,\nu'p)}{\overline{\sigma}(\nu,\nu'n)}, \quad \overline{R}_{\overline{\nu}} = \frac{\overline{\sigma}(\overline{\nu},\overline{\nu}'p)}{\overline{\sigma}(\overline{\nu},\overline{\nu}'n)} \quad (19)$$

agree within 1% with those values obtained for a fixed neutrino energy of $E_\nu = 200$ MeV for all values of the strange form factors discussed in this paper. Thus, the results for $\overline{R}$ are virtually indistinguishable from those shown in Fig. 4.

Produced predominantly by π decay, the LAMPF DIF neutrino beam is a mixture of neutrinos and antineutrinos, where the latter make up about 20% of the useful neutrino beam. The ratio of proton-to-neutron yields to be measured in the LAMPF experiment is therefore

$$\overline{R}_{\rm LAMPF} = \frac{0.8\overline{\sigma}(\nu,\nu'p) + 0.2\overline{\sigma}(\overline{\nu},\overline{\nu}'p)}{0.8\overline{\sigma}(\nu,\nu'n) + 0.2\overline{\sigma}(\overline{\nu},\overline{\nu}'n)} . \quad (20)$$

We have calculated this ratio $\overline{R}_{\rm LAMPF}$ for the representative range of strange form factors $F_2^s(0)$ and $G_s(0)$ within the continuum RPA approach as outlined above. Our results are shown in Fig. 5. The mixture of neutrinos and antineutrinos in the beam has two interesting con-

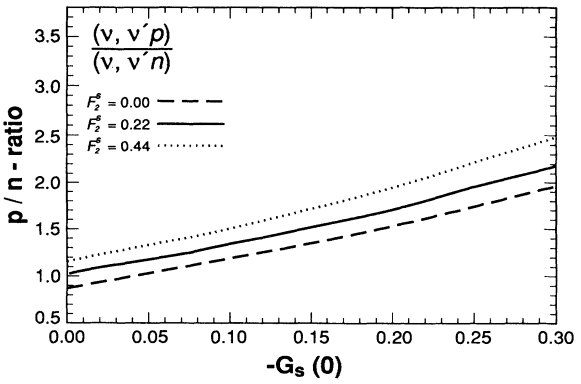

FIG. 5. Same as Fig. 4, but calculated for the LAMPF decay-in-flight neutrino beam.

sequences: First, the sensitivity of the ratio on $G_s(0)$ is slightly increased compared to the case of a pure neutrino beam, but, more importantly, the sensitivity of the ratio on $F_2^s(0)$ is largely reduced as the interference term, which is mainly responsible for the dependence of the ratio on the strange magnetic form factor, has different signs in $\bar{\nu}$- and ν-induced reactions. In fact, the ratio would be essentially independent of $F_2^s(0)$ for a neutrino beam consisting of 50% neutrinos and 50% antineutrinos.

Our continuum RPA calculation confirms that measuring the ratio of proton to neutron quasielastic yield appears to be a very promising way to determine the strange axial vector form factors of the nucleon. Importantly, we have demonstrated, by comparing the results of a mean-field approach with the one in which we considered final state interactions by a finite-range particle-hole residual interaction derived from the realistic Bonn potential, that the ratio is essentially independent of the adopted nuclear model. Thus, one can conclude from Fig. 5 that the LAMPF experiment will measure a ratio $\overline{R}_{\mathrm{LAMPF}} \gtrsim 1.2$, if the strange axial vector form factor is in fact as large as suggested in Ref. [4]. This ratio is significantly larger than the value obtained if the strange form factors $F_2^s(0)$ and $G_s(0)$ are both negligible ($\overline{R}_{\mathrm{LAMPF}} \approx 0.8$ in this case). The LAMPF experiment is expected to determine the ratio of proton-to-neutron yield with a statistical accuracy of better than 10%, and thus is clearly capable of directly and undoubtedly proving the existence of a strange axial vector form factor of the nucleon if $G_s(0) < -0.2$.

This research was supported in part by the National Science Foundation Grant Nos. PHY90-13248 and PHY91-15574, and the Office of Energy Research in the U.S. Department of Energy.

[1] H. Abramowicz *et al.*, CDHS Collaboration, Z. Phys. C **15**, 19 (1982).
[2] C. Foudas *et al.*, CCFR Collaboration, Phys. Rev. Lett. **64**, 1207 (1990).
[3] J. Gasser, H. Leutwyler, and M. E. Sainio, Phys. Lett. B **253**, 252 (1991); **253**, 260 (1991).
[4] J. Ashman *et al.*, EMC Collaboration, Nucl. Phys. **B328**, 1 (1989).
[5] R. L. Jaffe and A. Manohar, Nucl. Phys. **B337**, 509 (1990).
[6] G. T. Garvey, S. Krewald, E. Kolbe, and K. Langanke, Phys. Lett. B **289**, 249 (1992).
[7] D. Kaplan and A. Manohar, Nucl. Phys. **B310**, 527 (1988).
[8] J. Collins, F. Wilczek, and A. Zee, Phys. Rev. D **18**, 242 (1978).
[9] R. N. Mohapatra and G. Senjanvić, Phys. Rev. D **19**, 2165 (1979).
[10] L. Wolfenstein, Phys. Rev. D **19**, 3450 (1979).
[11] L. A. Ahrens *et al.*, Phys. Rev. D **35**, 785 (1987).
[12] E. J. Beise and R. D. McKeown, Comm. Nucl. Part. Phys. **20**, 105 (1991).
[13] G. T. Garvey, W. C. Louis, and D. H. White, Phys. Rev. C (in press).
[14] J. D. Walecka, in *Muon Physics*, edited by V. W. Hughes and C. S. Wu (Academic Press, New York, 1975), p. 113.
[15] E. Kolbe, K. Langanke, S. Krewald, and F. K. Thielemann, Nucl. Phys. **A540**, 599 (1992).
[16] M. Buballa, S. Drożdż, S. Krewald, and J. Speth, Ann. Phys. (N.Y.) **208**, 346 (1991).
[17] K. Nakayama, S. Drożdż, S. Krewald, and J. Speth, Nucl. Phys. **470**, 573 (1987).
[18] R. Machleidt, K. Holinde, and Ch. Elster, Phys. Rep. **149**, 1 (1987).
[19] M. Buballa, S. Drożdż, S. Krewald, and A. Szczurek, Phys. Rev. C **44**, 810 (1991).
[20] G. Co and S. Krewald, Phys. Lett. **137B**, 145 (1984).
[21] W. C. Louis, LSNC Collaboration, spokesman, LAMPF proposal 1173.
[22] R. L. Jaffe, Phys. Lett. B **229**, 275 (1989).
[23] F. Osterfeld, Rev. Mod. Phys. **64**, 491 (1992).